Available online at www.sciencedirect.com
ScienceDirect
Bioorganic & Medicinal Chemistry 16 (2008) 284–292
Bioorganic & Medicinal Chemistry

Discovery of novel α-glucosidase inhibitors based on the virtual screening with the homology-modeled protein structure

Hwangseo Park,[a,*] Kyo Yeol Hwang,[b] Kyung Hwan Oh,[b] Young Hoon Kim,[b] Jae Yeon Lee[b] and Keun Kim[b,*]

[a]*Department of Bioscience and Biotechnology, Sejong University, 98 Kunja-Dong, Kwangjin-Ku, Seoul 143-747, Republic of Korea*
[b]*Department of Bioscience and Biotechnology, The University of Suwon, San 2-2 Wau-ri, Bongdam-eup, Hwaseong-si, Gyeonggi-do 445-743, Republic of Korea*

Received 20 August 2007; revised 17 September 2007; accepted 19 September 2007
Available online 22 September 2007

Abstract—Discovery of α-glucosidase inhibitors has been actively pursued with the aim to develop therapeutics for the treatment of diabetes and the other carbohydrate mediated diseases. We have been able to identify 13 novel α-glucosidase inhibitors by means of a computer-aided drug design protocol involving homology modeling of the target protein and the virtual screening with docking simulations under consideration of the effects of ligand solvation in the binding free energy function. Because the newly discovered inhibitors are structurally diverse and reveal a significant potency with IC_{50} values lower than 50 μM, all of them can be considered for further development by structure–activity relationship studies or de novo design methods. Structural features relevant to the interactions of the newly identified inhibitors with the active site residues of α-glucosidase are discussed in detail.

1. Introduction

Glucosidases catalyze the final step in the digestive process of carbohydrates by the hydrolysis of a glycosidic bond in oligosaccharides. They are responsible for the catalytic cleavage of a glycosidic bond with specificity depending on the number of monosaccharides, the position of cleavage site, and the configuration of the hydroxyl groups in the substrate.[1] The most extensively studied are α- and β-glucosidases that are known to catalyze the hydrolysis of the glycosidic bonds involving a terminal glucose at the cleavage site through α- and β-linkages at the anomeric center. These two glucosidases differ in how to position their two carboxylic acid sidechains during catalysis[2]: one plays the role of a catalytic nucleophile attacking the anomeric center, and the other acts as an acid catalyst weakening the C–O bond by protonation. Of the two popular glucosidases, α-glucosidase (EC 3.2.1.20) has drawn a special interest of the pharmaceutical research community because it was shown in earlier studies that the inhibition of its catalytic activity resulted in the retardation of glucose absorption and the decrease in postprandial blood glucose level.[3–5] Therefore, effective α-glucosidase inhibitors may serve as chemotherapeutic agents for clinic use in the treatment of diabetes and obesity. Due to the catalytic role in digesting carbohydrate substrates, α-glucosidase has also been well appreciated as a therapeutic target for the other carbohydrate mediated diseases including cancer,[6] viral infections,[7,8] and hepatitis.[9]

Since the discovery of acarbose that is the first member of α-glucosidase inhibitors approved for the treatment of type 2 diabetes,[10] a variety of α-glucosidase inhibitors have been discovered as recently reviewed in an extensive fashion.[11] These include transition state analogues,[12] newly identified synthetic compounds,[13–20] and natural products isolated from a variety of species.[21–23] Most of the α-glucosidase inhibitors reported in the literature stem from either the isolation of new scaffolds by high throughput screening or the generation of the improved derivatives of pre-existing inhibitor scaffolds. So far the rational drug design protocol has not been applied for α-glucosidases because the

Keywords: α-glucosidase; Inhibitor; Virtual screening; Homology modeling; Enzyme assay; Docking; Diabetes.
* Corresponding authors. Tel.: +82 2 3408 3766; fax: +82 2 3408 3334 (H.P.); tel./fax: +82 31 220 2344 (K.K.); e-mail addresses: hspark@sejong.ac.kr; kkim@suwon.ac.kr

0968-0896/$ - see front matter © 2007 Elsevier Ltd. All rights reserved.
doi:10.1016/j.bmc.2007.09.036

structural investigations have lagged behind the mechanistic and pharmacological studies. Indeed, structural information of α-glucosidases has thus been limited to those of a few bacterial strains only in ligand-free forms.[24,25] The lack of structural information about the nature of the interactions between α-glucosidases and small molecule inhibitors has thus made it a difficult task to discover good lead compounds based on the structure-based inhibitor design.

In the present study, we identify the novel classes of α-glucosidase inhibitors by means of a drug-design protocol involving homology modeling, structure-based virtual screening with docking simulations, and in vitro enzyme assay in a consecutive manner. The characteristic feature that discriminates our virtual screening approach from the others lies in the implementation of an accurate solvation model in calculating the binding free energy between α-glucosidase and putative ligands, which would have the effect of increasing the hit rate in enzyme assay.[26,27] We selected the α-glucosidase from baker's yeast as the target protein in virtual screening because it had been used most extensively in biological assays to evaluate the newly discovered α-glucosidase inhibitors. To the best of our knowledge, we report the first example for the successful application of the structure-based virtual screening to identify novel α-glucosidase inhibitors. It will be shown that the docking simulation with the improved binding free energy function can be a useful tool for elucidating the observed activity of the identified inhibitors, as well as for enriching the chemical library used in screening assays with molecules that are likely to have biological activities.

2. Results and discussion

2.1. Homology modeling of α-glucosidase

Figure 1 displays the sequence alignment between α-glucosidase MAL12 from baker's yeast and oligo-1,6-glucosidase from *Bacillus cereus* (O16GB). According to this alignment, the sequence identity and the similarity amount to 38.5% and 58.4%, respectively. Judging from such a high sequence homology, a high-quality 3D structure of α-glucosidase can be expected in the homology modeling. It is indeed well known that a homology-modeled structure of a target protein can be accurate enough to be used in docking studies once the sequence identity between target and template approaches 40%.[28] Based on the sequence alignment shown in Figure 1, 10 structural models of α-glucosidase were calculated and the one with the lowest value of MODELLER objective function was selected as the final model to be used in the subsequent virtual screening.

Figure 2 shows the structure of α-glucosidase obtained from the homology modeling in comparison with the X-ray crystal structure of oligo-1,6-glucosidase that was used as the template. The target and the template possess a very similar folding structure and are superimposable over the main chain atoms. The two

```
MAL12     9  TEPKWWKEATIYQIYPASFKDSNNDGWGDLKGITSKLQYIKDLGVDAIWVCPFYDSPQQD  68
O16GB     1  MEKQWWKESVVYQIYPRSFMDSNGDGIGDLRGIISKLDYLKELGIDVIWLSPVYESPNDD  60

MAL12    69  MGYDISNYEKVWPTYGTNEDCFELIDKTHKLGMKFITDLVINHCSTEHEWFKESRSSKTN 128
O16GB    61  NGYDISDYCKIMNEFGTMEDWDELLHEMHERNMKLMMDLVVNHTSDEHNWFIESRKSKDN 120

MAL12   129  PKRDWFFWRPPKGYDAEGKPIPPNNWKSFFGGSAWTFDETTNEFYLRLFASRQVDLNWEN 188
O16GB   121  KYRDYYIWRPGK----EGK--EPNNWGAAFSGSAWQYDEMTDEYYLHLFSKKQPDLNWDN 174

MAL12   189  EDCRRAIFESAVGFWLDHGVDGFRIDTAGLYSKRPGLPDSPIFDKTSKLQHPNWGSHNGP 248
O16GB   175  EKVRQDVYEMMK-FWLEKGIDGFRMDVINFISKEEGLPTVETEEEGYVSGHKHF--MNGP 231

MAL12   249  RIHEYHQELHRFMKNRVKDGREIMTVGEVAHGS--DNALYTSAARYEVSEVFSFTHVEVG 306
O16GB   232  NIHKYLHEMN----EEVLSHYDIMTVGEMPGVTTEEAKLYTGEERKELQMVFQFEHMDLD 287

MAL12   307  TSPFFRYNIVPFTLKQWKEAIASNFLFINGTDSWATTYIENHDQARSITRFADDSPKYRK 366
O16GB   288  SGEGGKWDVKPCSLLTLKENLTKWQKALEHTG-WNSLYWNNHDQPRVVSRFGNDG-MYRI 345

MAL12   367  ISGKLLTLLECSLTGTLYVYQGQEIGQINFKEWPIEKYEDVDVKNNYEIIKKSFGKNSKE 426
O16GB   346  ESAKMLATVLHMMKGTPYIYQGEEIGMTNVRFESIDEYRDIETLN---MYKEKVMERGED 402

MAL12   427  MKDFFKGIALLSRDHSRTPMPWTKDKPNAGFTGPDVKPWFLLNESFEQGINVEQESRDDD 486
O16GB   403  IEKVMQSIYIKGRDNARTPMQWD-DQNHAGFT--TGEPWITVNPNYKE-INVKQAIQNKD 458

MAL12   487  SVLNFWKRALQARKKYKELMIYGYDFQFIDLDSDQIFSFTKEYEDKTLFAALNFSGEEIE 546
O16GB   459  SIFYYYKKLIELRKN-NEIVVYG-SYDLILENNPSIFAYVRTYGVEKLLVIANFTAEECI 516

MAL12   547  FSLPREG--ASLSFILGNYDDTD--VSSRVLKPWEGRIYLVK 584
O16GB   517  FELPEDISYSEVELLIHNYDVENGPIENITLRPYEAMVFKLK 558
```

Figure 1. Sequence alignment between α-glucosidase (MAL12) and oligo-1,6-glucosidase (O16GB). The identity and the similarity between the corresponding residues are indicated in red and green, respectively. The active site residues are indicated in a blue rectangular box.

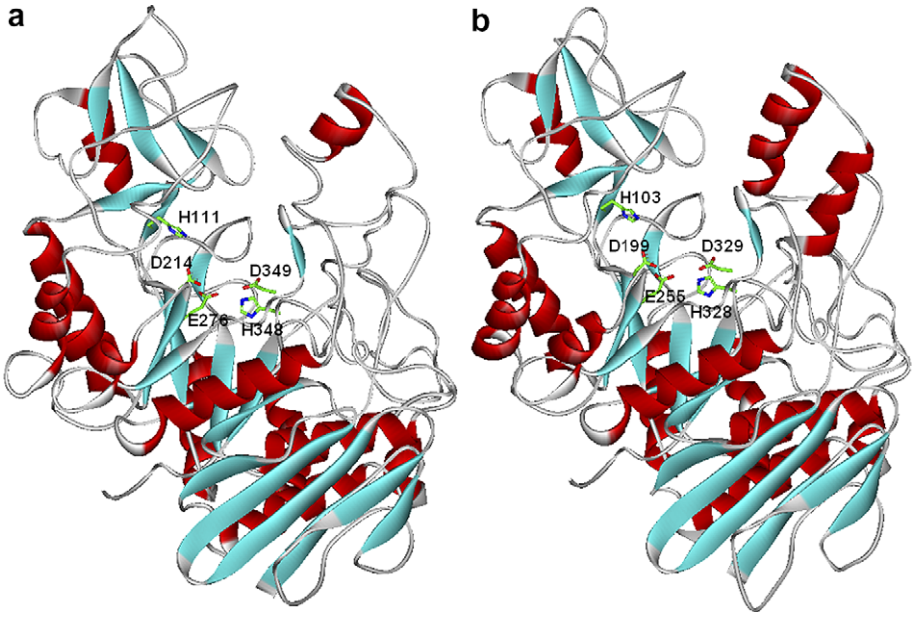

Figure 2. Comparative view of (a) homology-modeled structure of α-glucosidase and (b) X-ray crystal structure of oligo-1,6-glucosidase.

enzymes also share the catalytic residues that are situated in their respective active sites in a similar fashion. This is not surprising because both enzymes catalyze the hydrolysis of terminal glycosidic bond of carbohydrates.[29] However, α-glucosidase is more compact in amino acid packing than oligo-1,6-glucosidase due to the possession of 18 more amino acid residues in the alignment position. Such a structural difference may be related with the differentiations of the active site geometry and substrate specificity as well as the catalytic efficiency. Indeed, glucosidases have generally exhibited a high specificity in enzyme catalysis by cleaving only one type of glycosidic linkage in a given anomeric configuration.[30]

The final structural model of α-glucosidase obtained from homology modeling was tested with the ProSa 2003 program by examining whether the interaction of each residue with the remainder of the protein is maintained favorable. This program calculates the knowledge-based mean fields to judge the quality of protein folds and has been widely used to measure the stability of a protein conformation. Figure 3 shows the ProSa 2003 energy profile of the homology-modeled α-glucosidase in comparison to that of the X-ray structure of oligo-1,6-glucosidase. We note that the ProSa energy of α-glucosidase remains negative for all amino acid residues except for a few around the residue number 210, indicating the acceptability of the homology-modeled

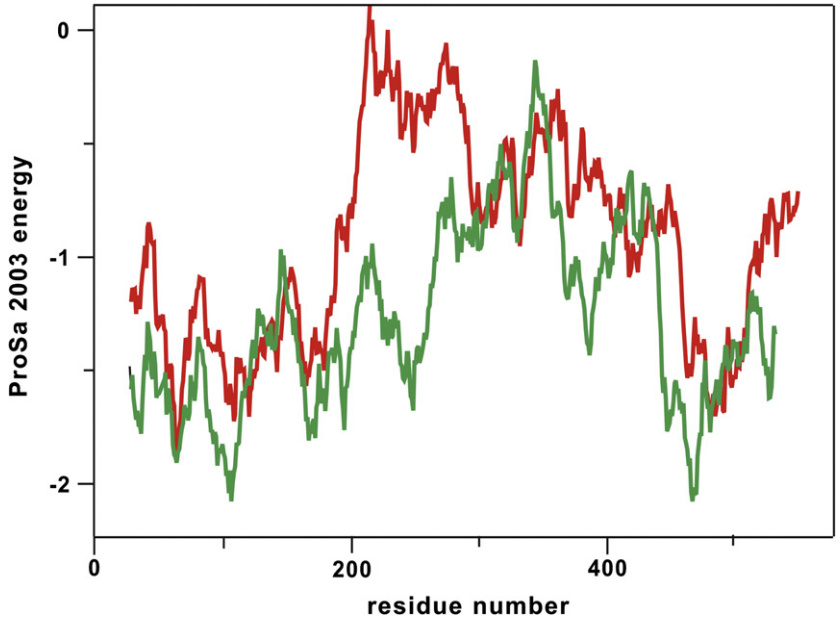

Figure 3. Comparison of the ProSa energy profiles for the homology-modeled structure of α-glucosidase (red) and the X-ray structure of oligo-1,6-glucosidase (green).

structure. This result supports the possibility that the homology modeling with a high sequence identity and a high-quality template structure can produce a 3D structure of target protein comparable in accuracy to that determined from X-ray crystallography.[28]

2.2. Virtual screening and in vitro α-glucosidase inhibition assay

Of the 85,000 compounds subject to the virtual screening with docking simulations, 200 top-scored compounds were selected as virtual hits. One hundred and eighty-eight of them were available from the compound supplier and were tested for inhibitory activity against the α-glucosidase from baker's yeast by in vitro enzyme assay. Among the 188 screened compounds, 13 revealed more than 50% inhibition at the concentration of 50 μM. The chemical structures and the inhibitory activities of these newly identified inhibitors are shown in Figure 4 and Table 1, respectively. Also, the physicochemical properties of these new α-glucosidase inhibitors are listed in Table 2 to provide insight into the estimation of their drug-likeness. To the best of our knowledge, these compounds have not been reported as α-glucosidase inhibitors so far in the literature and patents. It is also noted that the compounds shown in Figure 4 are structurally diverse, and each of them can be considered as a new inhibitor scaffold for further development by structure–activity relationship or de novo design studies.

2.3. Molecular modeling studies for the inhibitory mechanism

To obtain some energetic and structural insight into the inhibitory mechanisms of the identified inhibitors of α-glucosidase, their binding modes in the active site were investigated using the AutoDock program with the procedure described in Section 4. The calculated binding mode of **11** in the active site of α-glucosidase is shown in Figure 5. It is noted that the phenolic oxygen of the inhibitor receives and donates a hydrogen bond from the side chain of His348 and to that of Asp349, respectively. Because these two residues are believed to play a critical role in the catalytic mechanism as the corresponding residues of His328 and Asp329 in oligo-1,6-glucosidase,[29] the phenol moiety seems to be an effective chemical group for binding in the active site of α-glucosidase and thereby for inhibiting its catalytic activity. In this regard, chalcone and its derivatives possessing the phenol moiety have also been identified as one of the novel classes of α-glucosidase inhibitors,[20] which are not based on a sugar scaffold. A strong hydrogen bond is

Table 1. Inhibitory activities of the newly identified compounds **1**–**13** against α-glucosidase

Compound	% Inhibition at 50 μM
1	58.0 ± 4.3
2	62.4 ± 6.1
3	50.6 ± 1.1
4	54.0 ± 0.7
5	50.9 ± 3.8
6	59.2 ± 2.0
7	62.2 ± 4.9
8	66.5 ± 5.4
9	52.3 ± 0.6
10	61.4 ± 4.7
11	71.4 ± 4.9
12	70.1 ± 6.6
13	63.1 ± 7.8

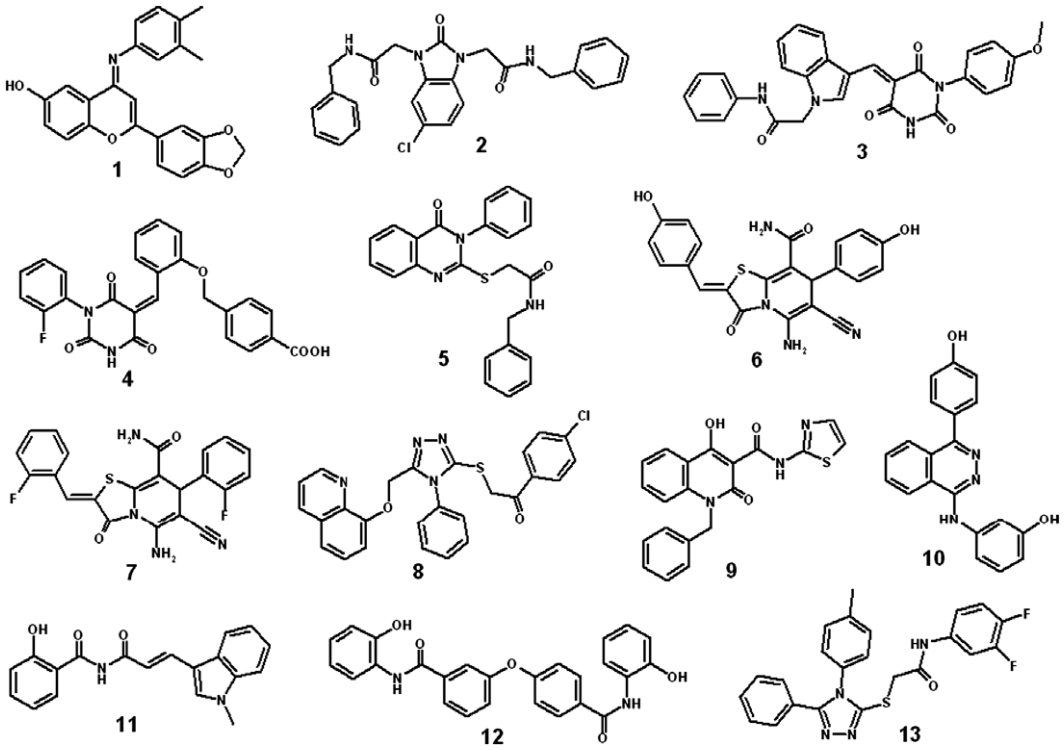

Figure 4. Chemical structures of the newly identified α-glucosidase inhibitors.

Table 2. Physicochemical properties of the newly identified α-glucosidase inhibitors

Compound	Molecular weight	Number of hydrogen bond donors	Number of hydrogen bond acceptors	Number of rotatable bonds	Clog *P*
1	385.4	1	5	2	4.64
2	462.9	2	7	10	4.86
3	494.5	2	9	7	3.19
4	460.4	2	8	6	3.62
5	401.5	1	5	7	3.52
6	432.5	4	8	4	1.09
7	436.4	2	6	4	2.71
8	487.0	0	6	8	5.18
9	377.4	2	6	5	3.78
10	329.4	3	5	3	4.43
11	320.4	2	5	5	4.73
12	440.5	4	7	8	4.38
13	436.5	1	5	7	5.18

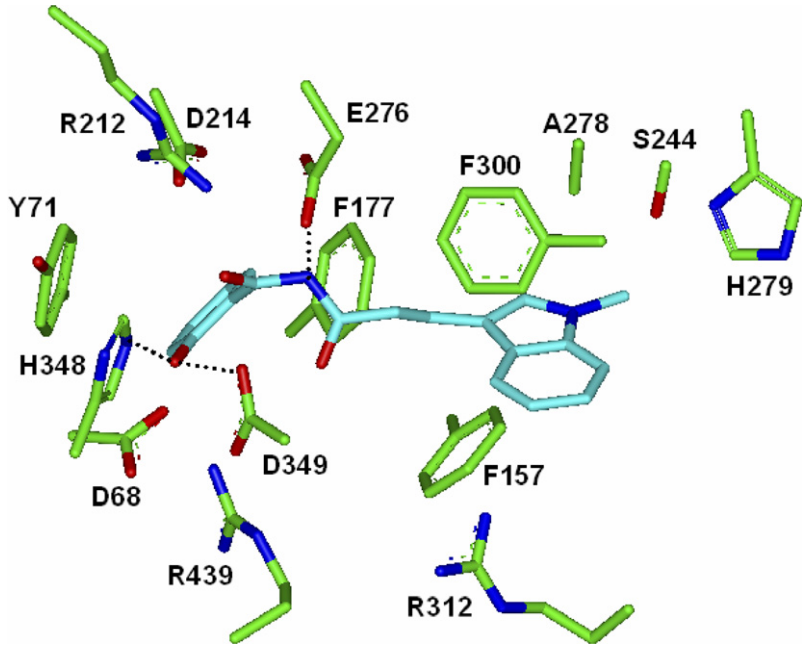

Figure 5. Binding mode of **11** in the active site of α-glucosidase. Carbon atoms of the protein and the ligand are indicated in green and cyan, respectively. Each dotted line indicates a hydrogen bond.

also established between the amidic nitrogen of the inhibitor and the side chain of Glu276. This interaction seems to be also important in the inhibition of α-glucosidase because Glu276 is the corresponding residue of Glu255, which is one of the catalytic residues of oligo-1,6-glucosidase.[29] Related with the pattern for hydrogen bond formation by inhibitor nitrogen, Tomich et al. reported a different binding mode in which a stable hydrogen bond was established between the nitrogen of glycosidic bridge of a pseudo-disaccharide inhibitor and Asp349.[31] The inhibitor **11** can be further stabilized in the active site by the hydrophobic interactions of the *N*-methyl indole moiety with the side chains of Phe157, Phe300, Ala278, Ser244, and His279. Judging from the structural features derived from docking simulations, the compound **11** should be capable of inhibiting the catalytic action of α-glucosidase by binding in the active site through the hydrogen bond and hydrophobic interactions in a cooperative fashion.

Figure 6 shows the lowest-energy AutoDock conformation of the compound **12** in the active site of α-glucosidase. As in the case of compound **11**, the phenolic oxygen of the inhibitor is hydrogen bonded to the catalytic residue of Asp349, confirming the importance of the phenol moiety for binding in the active site. This supports the possibility of the potential role of the inhibitor phenol group as a surrogate for the terminal monosaccharide of a substrate. Recent computational studies showed that the formation of a hydrogen bond with a catalytic residue would also be important in the inhibition of β-glucosidase.[32] The binding mode of **12** differs from that of **11** in that the hydrogen bonds with His348 and Glu276 are not observed. This is due most

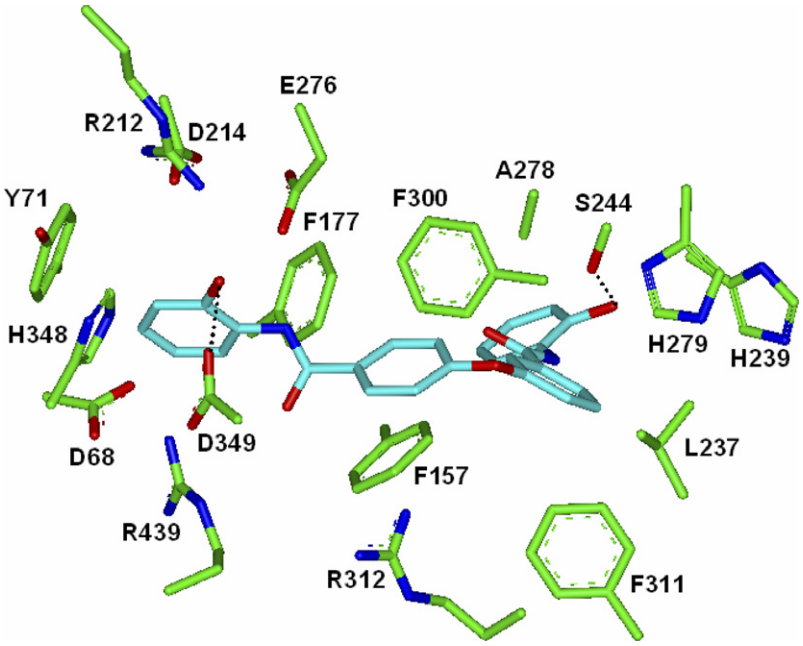

Figure 6. Binding mode of **12** in the active site of α-glucosidase. Carbon atoms of the protein and the ligand are indicated in green and cyan, respectively. Each dotted line indicates a hydrogen bond.

probably to the absence of the carbonyl group at the ortho position of the phenol group that can play the role of positioning the –OH and –NH groups of the inhibitor to form a hydrogen bond with the catalytic residues. However, an additional hydrogen bond is established between the second phenol moiety and Ser244 at the opposite side of the active site. Another characteristic feature that discriminates the binding mode of **12** from that of **11** is that the former is stabilized in the active site by more nonpolar side chains than the latter including Phe311 and Leu237. Thus, the strengthening of the hydrophobic interactions seems to compensate for the weakening of the hydrogen bond interactions, which can be an explanation for the similarity in inhibitory activities between the two inhibitors.

3. Conclusions

We have identified 13 new novel inhibitors of α-glucosidase by applying a computer-aided drug design protocol involving the homology modeling of the target protein and the structure-based virtual screening with docking simulations under consideration of the effects of ligand solvation in the binding free energy function. These inhibitors reveal a structural diversity as well as a significant potency with IC_{50} values lower than 50 μM. Therefore, each of the newly discovered inhibitors can provide a new scaffold for further development by structure–activity relationship studies or de novo design methods. Detailed binding mode analyses with docking simulation show that the inhibitors can be stabilized by the formation of hydrogen bonds with catalytic residues and the establishment of hydrophobic contacts at the opposite side of the active site.

4. Experimental

4.1. Homology modeling of yeast α-glucosidase

Although the X-ray crystal structures of a few bacterial α-glucosidases have been reported, structural information is still unavailable for the eukaryotic α-glucosidase enzymes commonly used in biological assays, such as that from baker's yeast. Therefore, we carried out homology modeling of α-glucosidase from baker's yeast to obtain its three-dimensional structure. This homology modeling started with the retrieval of the amino acid sequence of α-glucosidase MAL12 from baker's yeast that comprises 584 amino acid residues from the SWISS-PROT protein sequence data bank (http://www.expasy.org/sprot/; Accession No. P53341).[33] In order to find a proper structural template for homology modeling, we searched for the Protein Data Bank (PDB) at National Center for Biotechnology and Information (NCBI) using BLAST and PSIBLAST algorithms with the amino acid sequence of the target as input. The results showed that oligo-1,6-glucosidase from *B. cereus* reveals the highest sequence identity (38.5%) with the target. Therefore, its X-ray crystal structure (PDB ID: 1UOK)[29] was selected as the template for homology modeling. Although 4-α-glucanotransferase from *Thermotoga maritima* revealed a sequence identity of about 30% with the target protein, it was excluded in homology modeling because the number of aligned amino acids amounts to at the most 300 as compared to 575 in case of oligo-1,6-glucosidase from *B. cereus*.

Sequence alignment between α-glucosidase from baker's yeast and oligo-1,6-glucosidase from *B. cereus* was then derived with the ClustalW package[34] using the

BLOSUM matrices for scoring the alignments. The parameters of GAP OPEN, GAP EXTENTION, and GAP DISTANCE were set equal to 10, 0.05, 8, respectively. Opening and extension gap penalties were changed systematically, and the obtained alignment was inspected for violation of structural integrity in the structurally conserved regions. Based on the best-scored sequence alignment, the structure of α-glucosidase from baker's yeast was constructed using the MODELLER 6v2 program.[35] In this model building, we employed an optimization method involving conjugate gradients and molecular dynamics to minimize the violations of the spatial restraints. More specifically, the 3D structural model was obtained from the optimization of molecular probability density function. With respect to the structure of gap regions, the coordinates were built from a randomized and distorted structure that is located approximately between the two anchoring regions as implemented in MODELLER 6v2. To increase the accuracy of the calculated structure, the loop modeling was also performed with the enumeration algorithm.[36] In selecting the final model of the target from the various 3D structures generated in the homology modeling, we used the MODELLER objective function because it measures the extent of violation from the spatial restraints. Then, we calculated the conformational energy of the predicted structure of α-glucosidase with ProSa 2003 program[37] for the purpose of a final evaluation.

4.2. Virtual screening of α-glucosidase inhibitors

We used the AutoDock program[38] in the structure-based virtual screening of α-glucosidase inhibitors because the outperformance of its scoring function over those of the others had been shown in several target proteins.[39] The atomic coordinates of α-glucosidase obtained from the homology modeling were used as the receptor model in the virtual screening with docking simulations. A special attention was paid to assign the protonation states of the ionizable Asp, Glu, His, and Lys residues. The side chains of Asp and Glu residues were assumed to be neutral if one of their carboxylate oxygens pointed toward a hydrogen-bond accepting group including the backbone aminocarbonyl oxygen at a distance within 3.5 Å, a generally accepted distance limit for a hydrogen bond of moderate strength.[40] Similarly, the side chains of Lys residues were protonated unless the NZ atom was in a close proximity of a hydrogen-bond donating group. The same procedure was also applied to determine the protonation states of ND and NE atoms in the side chains of His residues.

The docking library for α-glucosidase comprising about 85,000 compounds was constructed from the latest version of the Interbioscreen chemical database (http://www.ibscreen.com) containing approximately 30,000 natural and 320,000 synthetic compounds. This selection was based on the drug-like filters that adopt only the compounds with physicochemical properties of potential drug candidates[41] and without reactive functional group(s). All of the compounds included in the docking library were then subjected to the Corina program to generate their three-dimensional atomic coordinates, followed by the assignment of Gasteiger–Marsili atomic charges.[42] AMBER force field parameters were assigned for calculating the van der Waals interactions and the internal energy of a ligand as implemented in the AutoDock program. Docking simulations with AutoDock were then carried out in the active site of α-glucosidase to score and rank the compounds in the docking library according to their calculated binding affinities.

In the actual docking simulation of the compounds in the docking library, we used the empirical AutoDock scoring function improved by the implementation of a new solvation model for a compound. The modified scoring function has the following form:

$$\begin{aligned}\Delta G_{\text{bind}}^{\text{aq}} = {} & W_{\text{vdW}} \sum_{i=1} \sum_{j>i} \left(\frac{A_{ij}}{r_{ij}^{12}} - \frac{B_{ij}}{r_{ij}^{6}} \right) \\ & + W_{\text{hbond}} \sum_{i=1} \sum_{j>i} E(t) \left(\frac{C_{ij}}{r_{ij}^{12}} - \frac{D_{ij}}{r_{ij}^{10}} \right) \\ & + W_{\text{elec}} \sum_{i=1} \sum_{j>i} \frac{q_i q_j}{\varepsilon(r_{ij}) r_{ij}} + W_{\text{tor}} N_{\text{tor}} \\ & + W_{\text{sol}} \sum_{i=1} S_i \left(\text{Occ}_i^{\max} - \sum_{j>i} V_j e^{-\frac{r_{ij}^2}{2\sigma^2}} \right) \end{aligned} \quad (1)$$

where $W_{\text{vdW}}, W_{\text{hbond}}, W_{\text{elec}}, W_{\text{tor}}$, and W_{sol} are the weighting factors of van der Waals, hydrogen bond, electrostatic interactions, torsional term, and desolvation energy of inhibitors, respectively. r_{ij} represents the interatomic distance, and A_{ij}, B_{ij}, C_{ij}, and D_{ij} are related to the depths of the potential energy well and the equilibrium separations between the two atoms. The hydrogen bond term has an additional weighting factor, $E(t)$, representing the angle-dependent directionality. With respect to the distance-dependent dielectric constant, $\varepsilon(r_{ij})$, a sigmoidal function proposed by Mehler and Solmajer[43] was used in computing the interatomic electrostatic interactions between the receptor protein and a ligand molecule. In the entropic term, N_{tor} is the number of sp^3 bonds in the ligand. In the desolvation term, S_i and V_i are the solvation parameter and the fragmental volume of atom i,[44] respectively, while $\text{Occ}_i^{\max}$ stands for the maximum atomic occupancy. In the calculation of molecular solvation free energy term in Eq. (1), we used the atomic parameters recently developed by Kang et al.[45] because those of the atoms other than carbon were unavailable in the current version of AutoDock. This modification of the solvation free energy term is expected to increase the accuracy in virtual screening, because the underestimation of ligand solvation often leads to the overestimation of the binding affinity of a ligand with many polar atoms.[27]

The docking simulation of a compound in the docking library started with the calculation of the three-dimensional grids of interaction energy for all of the possible atom types present in chemical database. These uniquely defined potential grids for the receptor protein were then used in common for docking simulations of all compounds in the docking library. As the center of the common grids in the active site, we used the center of mass

coordinates of the docked structure of the probe molecule, acarbose, whose binding mode had been known in the active site of 4-α-glucanotransferase that is closely similar in structure to the template (oligo-1,6-glucosidase) used in the homology modeling.[46] The calculated grid maps were of dimension $61 \times 61 \times 61$ points with the spacing of 0.375 Å, yielding a receptor model that includes atoms within 22.9 Å of the grid center. For each compound in the library, 10 docking runs were performed with the initial population of 50 individuals. Maximum number of generations and energy evaluation were set to 27,000 and 2.5×10^5, respectively.

4.3. In vitro α-glucosidase inhibition assay

As widely used, the commercially available α-glucosidase from baker's yeast (Sigma, G5003) was selected as the target protein in this study using *p*-nitrophenyl-α-D-glucopyranoside (Sigma, N1377) as the substrate. The compounds selected from the precedent virtual screening were purchased from InterBioScreen Ltd and dissolved in DMSO. The reason for this choice for solvent lies in that most of the test compounds were soluble and maintained stable in DMSO. The enzyme and the substrate were dissolved in 0.07 M potassium phosphate buffer with pH 6.8. Then, the enzymatic reaction mixture composed of 100 μl α-glucosidase (0.1 U/ml), 99 μl of 5 mM substrate, and 1 μl (10 mM/ml DMSO) of test compound was incubated at 37 °C for 30 min. The inhibitory activity of each test compound was determined by measuring the remaining activity of α-glucosidase at the concentration of 50 μM. The enzymatic activity was measured by the amount of the released product, *p*-nitrophenol, that was detected by spectrophotometer at the wavelength of 415 nm. For all test compounds, the inhibition assay was performed in duplicate.

Acknowledgments

The authors acknowledge the support from KISTI (Korea Institute of Science and Technology Information) under 'The Eighth Strategic Supercomputing Support Program' with Dr. Sang Min Lee as the technical supporter. The use of the computing system of the Supercomputing Center is greatly appreciated.

References and notes

1. Kimura, A.; Lee, J.-H.; Lee, I.-S.; Lee, H.-S.; Park, K.-H.; Chiba, S.; Kim, D. *Carbohydr. Res.* **2004**, *339*, 1035–1040.
2. Heightman, T. D.; Andrea, T.; Vasella, A. T. *Angew. Chem., Int. Ed.* **1999**, *38*, 750–770.
3. Robinson, K. M.; Begovic, M. E.; Rhinehart, B. L.; Heineke, E. W.; Ducep, J. B.; Kastner, P. R.; Marshall, F. N.; Danzin, C. *Diabetes* **1991**, *40*, 825–830.
4. Braun, C.; Brayer, G. D.; Withers, S. G. *J. Biol. Chem.* **1995**, *270*, 26778–26781.
5. Dwek, R. A.; Butters, T. D.; Platt, F. M.; Nicole Zitzmann, N. *Nat. Rev. Drug Disc.* **2002**, *1*, 65–75.
6. Humphries, M. J.; Matsumoto, K.; White, S. L.; Olden, K. *Cancer Res.* **1986**, *46*, 5215–5222.
7. Mehta, A.; Zitzmann, N.; Rudd, P. M.; Block, T. M.; Dwek, R. A. *FEBS Lett.* **1998**, *430*, 17–22.
8. Karpas, A.; Fleet, G. W. J.; Dwek, R. A.; Petursson, S.; Namgoong, S. K.; Ramsden, N. G.; Jacob, G. S.; Rademacher, T. W. *Proc. Natl. Acad. Sci. U.S.A.* **1988**, *85*, 9229–9233.
9. Zitzmann, N.; Mehta, A. S.; Carrouée, S.; Butters, T. D.; Platt, F. M.; McCauley, J.; Blumberg, B. S.; Dwek, R. A.; Block, T. M. *Proc. Natl. Acad. Sci. U.S.A.* **1999**, *96*, 11878–11882.
10. Yee, H. S.; Fong, N. T. *Pharmacotherapy* **1996**, *16*, 792–805.
11. de Melo, E. B.; Gomes, A. S.; Carvalho, I. *Tetrahedron* **2006**, *62*, 10277–10302.
12. Lillelund, V. H.; Jensen, H. H.; Liang, X.; Bols, M. *Chem. Rev.* **2002**, *102*, 515–553.
13. Xu, H.-W.; Dai, G.-F.; Liu, G.-Z.; Wang, J.-F.; Liu, H.-M. *Bioorg. Med. Chem.* **2007**, *15*, 4247–4255.
14. Tanabe, G.; Yoshikai, K.; Hatanaka, T.; Yamamoto, M.; Shao, Y.; Minematsu, T.; Muraoka, O.; Wang, T.; Matsuda, H.; Yoshikawa, M. *Bioorg. Med. Chem.* **2007**, *15*, 3926–3937.
15. Liu, Y.; Ma, L.; Chen, W.-H.; Wang, B.; Xu, Z.-L. *Bioorg. Med. Chem.* **2007**, *15*, 2810–2814.
16. Pandey, J.; Dwivedi, N.; Singh, N.; Srivastava, A. K.; Tamarkar, A.; Tripathi, R. P. *Bioorg. Med. Chem. Lett.* **2007**, *17*, 1321–1325.
17. Hakamata, W.; Nakanishi, I.; Masuda, Y.; Shimizu, T.; Higuchi, H.; Nakamura, Y.; Saito, S.; Urano, S.; Oku, T.; Ozawa, T.; Ikota, N.; Miyata, N.; Okuda, H.; Fukuhara, K. *J. Am. Chem. Soc.* **2006**, *128*, 6524–6525.
18. Dai, G.-F.; Xu, H.-W.; Wang, J.-F.; Liu, F.-W.; Liu, H.-M. *Bioorg. Med. Chem. Lett.* **2006**, *16*, 2710–2713.
19. Liu, H.; Sim, L.; Rose, D. R.; Pinto, B. M. *J. Org. Chem.* **2006**, *71*, 3007–3013.
20. Seo, W. D.; Kim, J. H.; Kang, J. E.; Ryu, H. W.; Curtis-Long, M. J.; Lee, H. S.; Yang, M. S.; Park, K. H. *Bioorg. Med. Chem. Lett.* **2005**, *15*, 5514–5516.
21. Luo, J.-G.; Wang, X.-B.; Ma, L.; Kong, L.-Y. *Bioorg. Med. Chem. Lett.* **2007**, *17*, 4460–4463.
22. Saludes, J. P.; Lievens, S. C.; Molinski, T. F. *J. Nat. Prod.* **2007**, *70*, 436–438.
23. Du, Z.-Y.; Liu, R.-R.; Shao, W.-Y.; Mao, X. P.; Ma, L.; Gu, L.-Q.; Huang, Z.-S.; Chan, A. S. C. *Eur. J. Med. Chem.* **2006**, *41*, 213–218.
24. Lodge, J. A.; Maier, T.; Liebl, W.; Hoffmann, V.; Sträter, N. *J. Biol. Chem.* **2003**, *278*, 19151–19158.
25. Rajan, S. S.; Yang, X.; Collart, F.; Yip, V. L. Y.; Withers, S. G.; Varrot, A.; Thompson, J.; Davies, G. J.; Anderson, W. F. *Structure* **2004**, *12*, 1619–1629.
26. Zou, X.; Sun, Y.; Kuntz, I. D. *J. Am. Chem. Soc.* **1999**, *121*, 8033–8043.
27. Shoichet, B. K.; Leach, A. R.; Kuntz, I. D. *Proteins* **1999**, *34*, 4–16.
28. Baker, D.; Sali, A. *Science* **2001**, *294*, 93–96.
29. Watanabe, K.; Hata, Y.; Kizaki, H.; Katsube, Y.; Suzuki, S. *J. Mol. Biol.* **1997**, *269*, 142–153.
30. Nishio, T.; Hakamata, W.; Kimura, A.; Chiba, S.; Takatsuki, A.; Kawachi, R.; Oku, T. *Carbohydr. Res.* **2002**, *337*, 629–634.
31. Tomich, C. H.; da Silva, P.; Carvalho, I.; Taft, C. A. *J. Comput. Aided Mol. Des.* **2005**, *19*, 83–92.
32. Zhou, J.-M.; Zhou, J.-H.; Meng, Y.; Chen, M.-B. *J. Chem. Theory Comput.* **2006**, *2*, 157–165.
33. Bairoch, A.; Apweiler, R. *Nucleic Acids Res.* **1999**, *27*, 49–54.
34. Thompson, J. D.; Higgins, D. G.; Gibson, T. J. *Nucleic Acids Res.* **1994**, *22*, 4673–4680.
35. Sali, A.; Blundell, T. L. *J. Mol. Biol.* **1993**, *234*, 779–815.
36. Fiser, A.; Do, R. K. G.; Sali, A. *Protein Sci.* **2000**, *9*, 1753–1773.

37. Sippl, M. J. *Proteins* **1993**, *17*, 355–362.
38. Morris, G. M.; Goodsell, D. S.; Halliday, R. S.; Huey, R.; Hart, W. E.; Belew, R. K.; Olson, A. J. *J. Comput. Chem.* **1998**, *19*, 1639–1662.
39. Park, H.; Lee, J.; Lee, S. *Proteins* **2006**, *65*, 549–554.
40. Jeffrey, G. A. *An Introduction to Hydrogen Bonding*; Oxford University Press: Oxford, 1997.
41. Lipinski, C. A.; Lombardo, F.; Dominy, B. W.; Feeney, P. J. *Adv. Drug Delivery Rev.* **1997**, *23*, 3–25.
42. Gasteiger, J.; Marsili, M. *Tetrahedron* **1980**, *36*, 3219–3228.
43. Mehler, E. L.; Solmajer, T. *Protein Eng.* **1991**, *4*, 903–910.
44. Stouten, P. F. W.; Frömmel, C.; Nakamura, H.; Sander, C. *Mol. Simul.* **1993**, *10*, 97–120.
45. Kang, H.; Choi, H.; Park, H. *J. Chem. Inf. Model.* **2007**, *47*, 509–514.
46. Roujeinikova, A.; Raasch, C.; Sedelnikova, S.; Liebl, W.; Rice, D. W. *J. Mol. Biol.* **2002**, *321*, 149–162.